Article

Electronic Coupling in Tetraanisylarylenediamine Mixed-Valence Systems: The Interplay between Bridge Energy and Geometric Factors

Christoph Lambert, Chad Risko, Veaceslav Coropceanu, Jrgen Schelter, Stephan Amthor, Nadine E. Gruhn, Jason C. Durivage, and Jean-Luc Brdas

J. Am. Chem. Soc., **2005**, 127 (23), 8508-8516• DOI: 10.1021/ja0512172 • Publication Date (Web): 20 May 2005

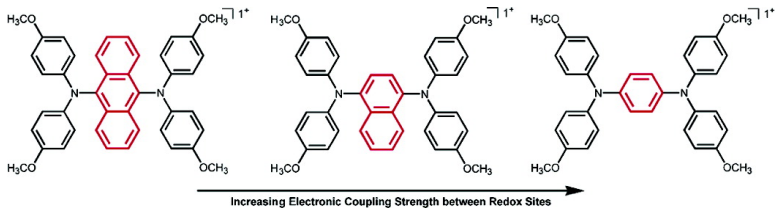

More About This Article

Additional resources and features associated with this article are available within the HTML version:

- Supporting Information
- Links to the 7 articles that cite this article, as of the time of this article download
- Access to high resolution figures
- Links to articles and content related to this article
- Copyright permission to reproduce figures and/or text from this article

View the Full Text HTML

J|A|C|S
ARTICLES
Published on Web 05/20/2005

Electronic Coupling in Tetraanisylarylenediamine Mixed-Valence Systems: The Interplay between Bridge Energy and Geometric Factors

Christoph Lambert,*,† Chad Risko,‡ Veaceslav Coropceanu,*,‡ Jürgen Schelter,† Stephan Amthor,† Nadine E. Gruhn,§ Jason C. Durivage,§ and Jean-Luc Brédas*,‡

Contribution from the Institut für Organische Chemie, Julius-Maximilians-Universität Würzburg, Am Hubland, D-97074 Würzburg, Germany, School of Chemistry and Biochemistry and Center for Organic Photonics and Electronics, Georgia Institute of Technology, 770 State Street, Atlanta, Georgia 30332-0400, and Department of Chemistry, The University of Arizona, 1306 East University Boulevard, Tucson, Arizona 85721-0041

Received February 25, 2005; E-mail: lambert@chemie.uni-wuerzburg.de; veaceslav.coropceanu@chemistry.gatech.edu; jean-luc.bredas@chemistry.gatech.edu

Abstract: We have investigated three organic mixed-valence systems that possess nearly identical inter-redox site distances and differ by the nature of the bridging units benzene, naphthalene, and anthracene: the *N*,*N*,*N*′,*N*′-tetra(4-methoxyphenyl)-1,4-phenylenene-diamine radical cation (**1**$^+$), the 1,4-bis(*N*,*N*-di(4-methoxyphenyl)-amino)naphthalene radical cation (**2**$^+$), and the 9,10-bis(*N*,*N*-di(4-methoxyphenyl)amino)-anthracene radical cation (**3**$^+$). The electronic interactions in these systems have been studied by means of gas-phase ultraviolet photoelectron spectroscopy, vis/NIR spectroscopy, and electronic-structure calculations. The experimental and theoretical results concur to indicate that the strength of electronic interaction decreases in the following order of bridging units: benzene > naphthalene > anthracene. This finding contradicts the usual expectation that anthracene is superior to benzene as a driving force for electronic communication. We explain these results in terms of a super-exchange mechanism and its strong dependence on steric interactions.

I. Introduction

The understanding of electron transfer (ET) through a bridging (B) molecular unit inserted either in a donor−bridge−acceptor triad or, in the case of molecular electronics, between nano-electrodes is of fundamental importance in many branches of chemistry, biology, and physics and in the design of high-performance molecular devices. In this context, mixed-valence (MV) systems, M−B−M$^+$, where the electron donor and acceptor sites (M and M$^+$, respectively) differ only by their charge (i.e., their oxidation state) have attracted much interest as simple model systems.[1−5]

While many issues regarding the influence of the bridge on the extent of electronic communication between the redox sites are well-studied (e.g., the role of the bridge length, topology, and energetics), the impact on electronic coupling of the interplay between different factors is still not well-understood. For instance, one well-established expectation is that anthracene as a bridging unit provides better electronic communication than benzene. Indeed, previous results reported by several groups[6−15] support this assumption and show that the replacement of a benzene spacer by anthracene significantly enhances the electronic communication in both charge[6−13] and energy[14,15] transfer systems. Thus, much larger electronic couplings have been found through 9,10-diethynylanthracene bridges than through 1,4-diethynylbenzene spacers in both inorganic[6] and purely organic[8,9] MV compounds as well as in single-molecule break junctions.[16] Furthermore, 9,10-diethynylanthracene has been shown to yield the largest electronic coupling between porphyrin

† Julius-Maximilians-Universität Würzburg.
‡ Georgia Institute of Technology.
§ The University of Arizona.

(1) Demadis, K. D.; Hartshorn, C. M.; Meyer, T. J. *Chem. Rev.* **2001**, *101*, 2655−2685.
(2) Barbara, P. F.; Meyer, T. J.; Ratner, M. A. *J. Phys. Chem.* **1996**, *100*, 13148−13168.
(3) Launay, J. P. *Chem. Soc. Rev.* **2001**, *30*, 386−397.
(4) Brunschwig, B. S.; Creutz, C.; Sutin, N. *Chem. Soc. Rev.* **2002**, *31*, 168−184.
(5) Coropceanu, V.; Andre, J. M.; Malagoli, M.; Brédas, J. L. *Theor. Chem. Acc.* **2003**, *110*, 59−69.
(6) Karafiloglou, P.; Launay, J. P. *Chem. Phys.* **2003**, *289*, 231−242.
(7) Fraysse, S.; Coudret, C.; Launay, J. P. *J. Am. Chem. Soc.* **2003**, *125*, 5880−5888.
(8) Lambert, C.; Nöll, G.; Schelter, J. *Nat. Mater.* **2002**, *1*, 69−73.
(9) Lambert, C.; Amthor, S.; Schelter, J. *J. Phys. Chem. A* **2004**, *108*, 6474−6486.
(10) Nelsen, S. F.; Ismagilov, R. F.; Powell, D. R. *J. Am. Chem. Soc.* **1996**, *118*, 6313−6314.
(11) Nelsen, S. F.; Ismagilov, R. F.; Powell, D. R. *J. Am. Chem. Soc.* **1997**, *119*, 10213−10222.
(12) Nelsen, S. F.; Ismagilov, R. F.; Powell, D. R. *J. Am. Chem. Soc.* **1998**, *120*, 1924−1925.
(13) Nelsen, S. F.; Ismagilov, R. F.; Gentile, K. E.; Powell, D. R. *J. Am. Chem. Soc.* **1999**, *121*, 7108−7114.
(14) Taylor, P. N.; Wylie, A. P.; Huuskonen, J.; Anderson, H. L. *Angew. Chem., Int. Ed.* **1998**, *37*, 986−989.
(15) Piet, J. J.; Taylor, P. N.; Anderson, H. L.; Osuka, A.; Warman, J. M. *J. Am. Chem. Soc.* **2000**, *122*, 1749−1757.
(16) Mayor, M.; Weber, H. B.; Reichert, J.; Elbing, M.; von Hanisch, C.; Beckmann, D.; Fischer, M. *Angew. Chem., Int. Ed.* **2003**, *42*, 5834−5838.

10.1021/ja0512172 CCC: $30.25

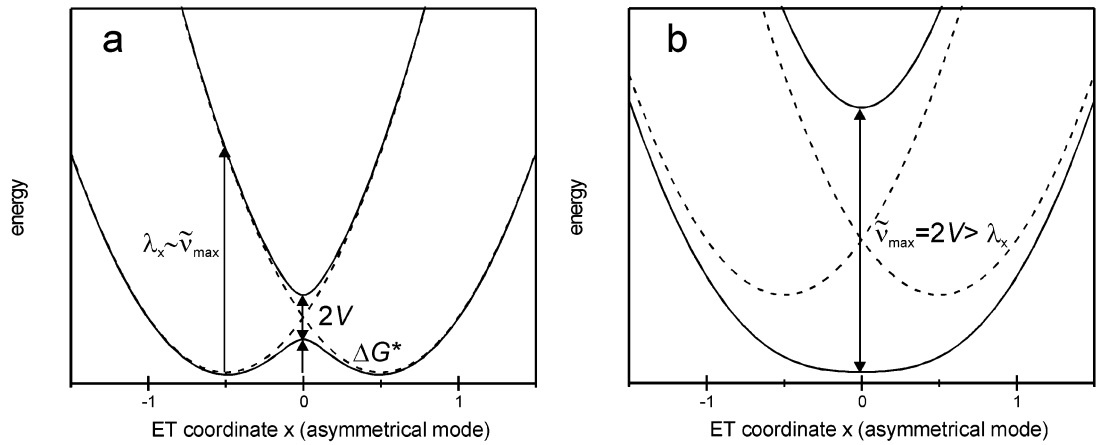

Figure 1. Diabatic potentials (dashed lines) and adiabatic potentials (solid lines) for a localized system (a) and a delocalized system (b) along the asymmetrical *x* mode.

chromophores.[14,15] Recent electron spin resonance (ESR) studies of bishydrazine compounds indicate significantly lower ET barriers for systems with anthracene linkers than for those with benzene and naphthalene bridges,[10−13] thus highlighting the efficient role of anthracene bridges in mediating electronic communication.

In this work, we describe the electronic structure of a series of bis[*N*,*N*-di-(4-methoxyphenyl)amino]arenes **1**−**3**, where the arene varies from benzene to naphthalene and anthracene:

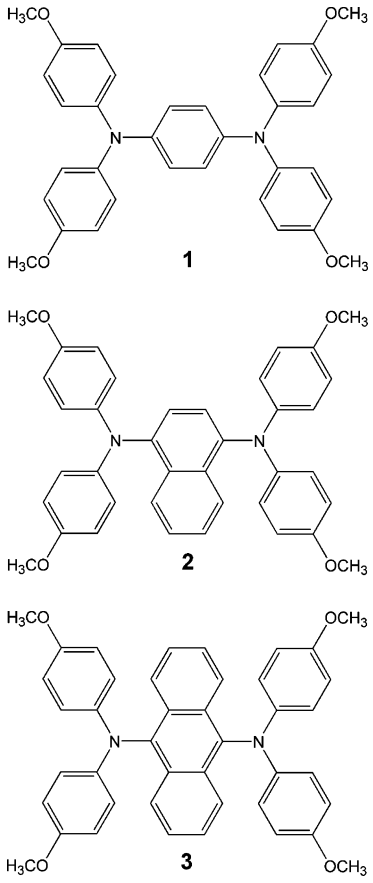

To understand the properties of these compounds, we have performed a series of quantum-chemical calculations and carried out a comprehensive series of measurements, including gas-phase ultraviolet photoelectron spectroscopy, vis-NIR, and cyclic voltammetry. In contrast to the previous findings on the role of arylene molecular bridges,[8−16] we provide evidence herein that, in the case of tetraanisylarylenediamine mixed-valence systems, the opposite trend holds (i.e., the electronic coupling is found to decrease on going from benzene to anthracene bridges). Our studies reveal that the efficiency of electronic communication depends on a subtle interplay between geometric and energetic factors.

II. Theoretical Model

We have considered the following model for the potential energy surfaces in the description of the electronic coupling and of its implications for the optical properties. The electronic mixing of the two diabatic states Ψ_a and Ψ_b, which correspond to the two valence structures $M_a^+-B-M_b$ and $M_a-B-M_b^+$ (i.e., the structures with the electron localized on the redox center on the right-hand side and on the left-hand side, respectively), leads to two adiabatic surfaces (see Figure 1). In accordance with the common Robin and Day classification, MV systems are divided into three classes: Class I, complete valence trapping (negligible electronic coupling between the two redox sites); Class II, valence trapping (weak electronic coupling); and Class III, delocalized valency (strong electronic coupling).[17] In the case of two degenerate diabatic states, the resulting adiabatic ground-state surface along the asymmetric ET coordinate (*x* mode) can display either a double minimum (Class II) when the electronic coupling 2*V* is smaller than the Marcus reorganization energy λ (Figure 1a) or a single minimum (Class III) for 2*V* greater than λ (Figure 1b). Optical excitation from the ground state to the excited state usually occurs in the near-infrared and is referred to as an intervalence charge-transfer (IV-CT) band.[18] The electronic-structure calculations discussed in the next section reveal that the electronic states related to the lowest optical transition in $\mathbf{1}^+-\mathbf{3}^+$ can be represented as linear combinations of two localized orbitals, each centered on one nitrogen atom. Moreover, the transition dipole moment of this band is polarized along the nitrogen−nitrogen axis, which is precisely what one would expect for a CT transition related to electron-transfer oscillations along this axis. These results

(17) Robin, M. B.; Day, P. *Advances in Inorganic Chemistry and Radiochemistry*; Academic Press: New York, 1967; Vol. 10, p 247.
(18) Charge-resonance (CR) is an alternative name for this band, especially used in the case of Class III systems.

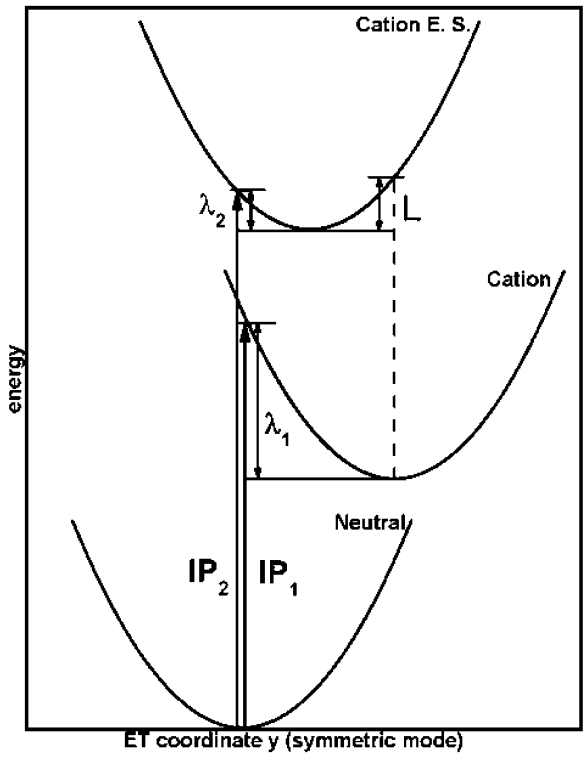

Figure 2. Adiabatic potential surfaces along the symmetric vibrational mode *y* (the *x* mode is set to zero) of the neutral state, and radical-cation ground and first excited states.

support the assignment of the lowest optical band in $\mathbf{1}^{+}-\mathbf{3}^{+}$ as an IV-CT transition and the assignment of these systems as mixed valent. As Hush and others have shown,[19−23] in addition to the averaged asymmetric mode, the symmetric mode (*y*), with reorganization energy *L*, can become important in describing the shape of the absorption band in delocalized systems (see Figure 2). Hush also showed how the IV-CT band can be used to estimate both the electronic coupling and the reorganization energy.[24,25] For the analysis of the IV-CT bands, we have employed here an extended two-state/two-mode model.

The geometries of **1**−**3** were optimized in the neutral and ground and first-excited radical-cation states. Density functional theory (DFT) and the semiempirical Hartree−Fock Austin Model 1 (RHF-AM1) method were utilized to evaluate the neutral states of the systems. The DFT calculations were carried out using the B3LYP functionals, where Becke's three-parameter hybrid exchange functional is combined with the Lee−Yang−Parr correlation functional,[26,27] with a 6-31G** split valence plus double polarization basis set.

UB3LYP/6-31G**, UHF-AM1, and a coupled semiempirical RHF-AM1/configuration interaction (AM1/CI) method using complete active space configuration interaction (CAS-CI) were used for the investigations of the radical-cation electronic states;

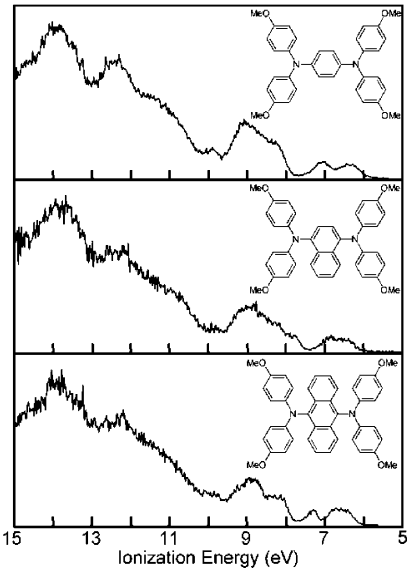

Figure 3. Gas-phase photoelectron spectra of **1**−**3**.

UB3LYP/6-31G** was used for the description of the first excited radical-cation state. Relaxation energies were determined through direct calculation of the relevant points on the potential energy surface, as discussed below.[28] Excitation energies for the low-lying excited states have been calculated with time-dependent density functional theory (TD-DFT). All AM1-based calculations were carried out using the implementation in the AMPAC 6.55 software package,[29] while the DFT calculations were performed with Gaussian98.[30]

The details of the synthesis and the procedures of the acquisition of the photoelectron, vis-NIR, and electrochemistry data are given in the Supporting Information.

III. Results and Discussion

Photoelectron Spectroscopy. The photoelectron spectra of **2** and **3**, along with the previously reported[31] spectrum of **1**, are shown in Figure 3, with the high-resolution close-up of the first ionizations given in Figure 4. The ionization potentials as derived from deconvolutions with Gaussian functions are given in Table 1. While the first ionization potential (IP1) slightly increases for **1**−**3**, the second ionization potential (IP2) displays some moderate decrease. This leads to a decrease in $\Delta IP = IP2 - IP1$, which goes from 0.69 eV (**1**) to 0.44 eV (**2**) and 0.34 eV (**3**). In strong contrast, the third ionization potential (IP3) strongly decreases from ca. 8.3 eV for **1** to 7.28 eV for **3**; we will show that this is indicative of the role of localized bridge states.

Redox Potentials. The redox potentials of **1**−**3**, measured by cyclic voltammetry in CH_2Cl_2, are given versus ferrocene in Table 2. Each of the compounds displays a reversible behavior for the first and second oxidations. The redox potential splitting ΔE between the first and second oxidation can be related to the electronic coupling in triarylamine mixed-valence systems.[32]

(19) Hush, N. S. In *Mixed-Valence Compounds: Theory and Applications in Chemistry, Physics, Geology, and Biology*; Proceedings of the NATO Advanced Study Institute, Oxford, England, Sept 9−21, 1979; Brown, D. B., Ed.; D. Reidel: Dordrecht, Holland, 1980; p 519.
(20) Reimers, J. R.; Hush, N. S. *Chem. Phys.* **1996**, *208*, 177−193.
(21) Piepho, S. B. *J. Am. Chem. Soc.* **1988**, *110*, 6319−6326.
(22) Piepho, S. B. *J. Am. Chem. Soc.* **1990**, *112*, 4197−4206.
(23) Coropceanu, V.; Malagoli, M.; Andre, J. M.; Brédas, J. L. *J. Am. Chem. Soc.* **2002**, *124*, 10519−10530.
(24) Hush, N. S. *Prog. Inorg. Chem.* **1967**, *8*, 391−443.
(25) Hush, N. S. *Coord. Chem. Rev.* **1985**, *64*, 135−157.
(26) Becke, A. D. *Phys. Rev. A: At., Mol., Opt. Phys.* **1988**, *38*, 3098−3100.
(27) Becke, A. D. *J. Chem. Phys.* **1993**, *98*, 5648−5652.
(28) Brédas, J. L.; Beljonne, D.; Coropceanu, V.; Cornil, J. *Chem. Rev.* **2004**, *104*, 4971−5003.
(29) *AMPAC 6.55*; Semichem: Shawnee, KS, 1997.
(30) Frisch, M. J. et al. *Gaussian98*, Rev. A.11; Gaussian, Inc.: Pittsburgh, PA, 1998.
(31) Coropceanu, V.; Gruhn, N. E.; Barlow, S.; Lambert, C.; Durivage, J. C.; Bill, T. G.; Nöll, G.; Marder, S. R.; Brédas, J. L. *J. Am. Chem. Soc.* **2004**, *126*, 2727−2731.
(32) Lambert, C.; Nöll, G. *J. Am. Chem. Soc.* **1999**, *121*, 8434−8442.

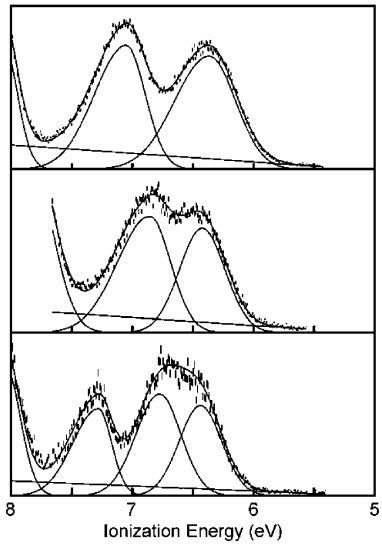

Figure 4. High-resolution close-up of the first ionizations of **1**−**3** with deconvolution by Gaussian functions.

Table 1. Ionization Potentials and Widths (between Brackets) of the Ionization Bands from Gas-Phase Photoelectron Spectra of **1**−**3**[a]

	IP1	IP2	IP3
1	6.36 (0.59)	7.05 (0.49)	ca. 8.3
2	6.42 (0.44)	6.86 (0.52)	ca. 7.9
3	6.44 (0.41)	6.78 (0.44)	7.28 (0.38)

[a] All values are in electronvolts.

Table 2. Redox Potentials of **1**−**3** in CH_2Cl_2/0.1 M TBAH vs Ferrocene When Applying a 250 mV s^{-1} Scan Rate

	$E_{1/2}^{ox,1}$/mV	$E_{1/2}^{ox,2}$/mV	$E_{1/2}^{ox,3}$/mV	ΔE
1	−145	340		495
2	60	320		260
3	220	310	1120[a]	90

[a] Irreversible process.

For **1**−**3**, ΔE decreases in going from **1** to **2** and **3**, in qualitative agreement with the UPS data.

Absorption Spectra. For all radical cations of $\mathbf{1}^+$−$\mathbf{3}^+$, an intense and asymmetric band appears in the NIR, which we assign to a charge-resonance (CR) band (see Figure 5). The transition moments (Table 3) of these bands were obtained by deconvolution of the CR band with two or three Gaussian functions. The band position, band shape, extinction coefficient ϵ, and transition moment μ are only slightly dependent on the solvent, which indicates that there is no net transfer of charge upon optical excitation. The molar absorptivity of $\mathbf{3}^+$ in MeCN could not be determined accurately as the radical cation slowly decomposes. The energy of the CR band decreases in the order $\mathbf{1}^+$ to $\mathbf{3}^+$ (see Table 3 for details). For $\mathbf{3}^+$, there is a prominent second band around 13 000 cm^{-1} that has a fine structure; this band shows features typical of a localized excitation in an anthracene radical cation.[33] The solvent-dependent shape of this band is reminiscent of the one observed in an anthracene radical cation substituted with two triarylamine-ethynylene groups.[9]

Geometries. Calculated key geometric parameters for the neutral and ground and first excited radical-cation states of **1**−**3**, as well as the X-ray crystal structure analysis of **3**, are collected in the Supporting Information. The B3LYP/6-31G** results for the neutral structures of **1**−**3** indicate that the geometries for the three systems are comparable, with the most prevalent deviations among the structures due to the asymmetric substitution of the naphthylene bridge in compound **2**; the theoretical evaluation of **3** compares very well with the experimental X-ray crystallographic determination. The carbon−carbon bond lengths of the phenylene and anthrylene bridges in **1** and **3** are symmetric about the nitrogen−nitrogen axes, while the asymmetric substitution of the naphthylene bridge lowers the symmetry normally realized for isolated naphthalene structures.

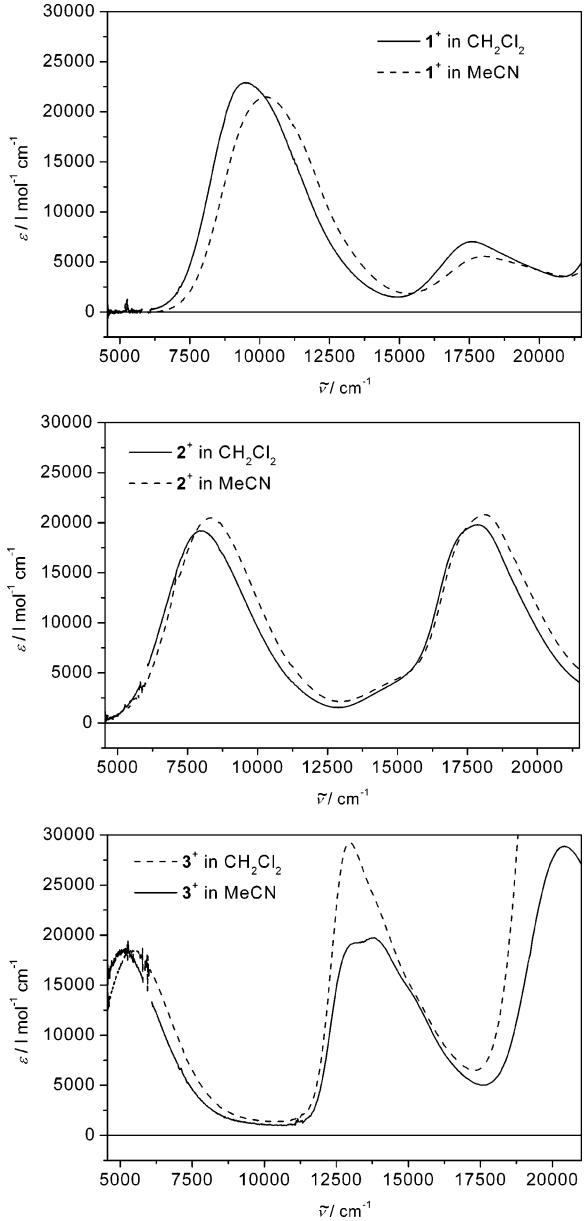

Figure 5. Vis/NIR spectra of $\mathbf{1}^+$−$\mathbf{3}^+$ in CH_2Cl_2 and in MeCN.

Table 3. Experimental Data for the Lowest Optical Band of $\mathbf{1}^+$−$\mathbf{3}^+$

	$\tilde{\nu}_{abs}$/cm^{-1}		ϵ/M^{-1} cm^{-1}		μ/D	
	CH_2Cl_2	MeCN	CH_2Cl_2	MeCN	CH_2Cl_2	MeCN
$\mathbf{1}^+$	9480	10180	22800	21460	9.3	8.9
$\mathbf{2}^+$	8000	8330	19100	20500	9.0	9.3
$\mathbf{3}^+$	5140	5450	18500		9.8	

(33) Shida, T. *Electronic Absorption Spectra of Radical Ions*; Elsevier: Amsterdam, 1988; p 446.

The larger anthrylene bridge of **3**, through increased steric interactions, produces a large torsional orientation of the *N*,*N*-di(4-methoxyphenyl)amino groups with respect to the bridge (72° for **3** versus 39° for **1**); these torsion angles represent the dihedral angles between the plane defined by the arylene bridge and that defined by the three carbon−nitrogen bonds around the redox site (see the Supporting Information). The theoretical estimates of the dihedral angles are in qualitative agreement with the experimental values of 72° and 74° for **3**, and 54° and 56° for tetraphenylphenylenediamine, a structural analogue of **1**.[34] The asymmetric substitution in **2** causes the torsional angles around each redox center to be 49° and 67° (values between those observed for the phenylene and anthrylene bridges of **1** and **3**), while X-ray crystal structure determination with very high *R* values gives 35−48° and 62−67° for eight total independent torsional angles. These torsional angles reveal the different landscapes of the 4-methoxyphenyl groups with respect to the naphthylene bridge: one unit is free from steric interactions with the bridge (as with the phenylene bridge) while the other group is hindered by increased steric interactions (as with the anthrylene bridge). Comparable geometries for **1**−**3** are realized at the RHF-AM1 level. The largest departure with respect to the B3LYP/6-31G** results occurs for the orientation of the nitrogen atoms; in all three systems at the RHF-AM1 level, the nitrogen atoms are pyramidal with respect to their bound carbon atoms, with the pyramidality in **2** being slightly larger.

Geometry optimizations of the radical-cation structures $\mathbf{1}^+$−$\mathbf{3}^+$ at the UB3LYP/6-31G** level of theory indicate that all three radical cations possess the same degrees of symmetry as their neutral structures. The bonds between the nitrogens and the bridge carbons shorten considerably in $\mathbf{1}^+$−$\mathbf{3}^+$, with the extent of change larger for $\mathbf{1}^+$ (0.028 Å) and $\mathbf{2}^+$ (0.025 Å) versus $\mathbf{3}^+$ (0.015 Å). Because of the decrease in these bond lengths, the distance between the two nitrogen redox centers decreases by 0.053, 0.043, and 0.024 Å, for $\mathbf{1}^+$, $\mathbf{2}^+$, and $\mathbf{3}^+$, respectively. The largest geometric adjustments to the overall radical-cation structures occur for the relative orientation of the 4-methoxyphenyl groups with respect to the bridges. In $\mathbf{1}^+$ and $\mathbf{3}^+$, the geometry relaxations decrease the torsional angles by 10° and 12°, respectively, while the nitrogen atoms remain non-pyramidal with respect to their bridging carbon atoms. The torsional orientation of the 4-methoxyphenyl groups with respect to the naphthylene bridge in $\mathbf{2}^+$ decreases by 17° for the more sterically hindered group and 9° for the less hindered group. It is worth noting that there is a slight diagonal twisting in the naphthylene and anthrylene bridges of $\mathbf{2}^+$ and $\mathbf{3}^+$.

The symmetric, delocalized structures provided by the UB3LYP/6-31G** method are consistent with DFT results reported for other triarylamine-based mixed-valence systems. However, such symmetric structures are provided by DFT even in the case of systems that are experimentally known to localize the excess charge.[23,35] To search for possible charge-localized structures, UHF-AM1 and correlated semiempirical AM1/CI methods were used. The UHF-AM1 results indicate that the charge is localized on one side of the molecular architecture for $\mathbf{2}^+$ and $\mathbf{3}^+$; the results are less clear for $\mathbf{1}^+$. However, each UHF-AM1-optimized structure was associated with a large degree of spin contamination ($S^2 \approx 1.8$−3.2), thus casting strong doubt on the validity of the method.

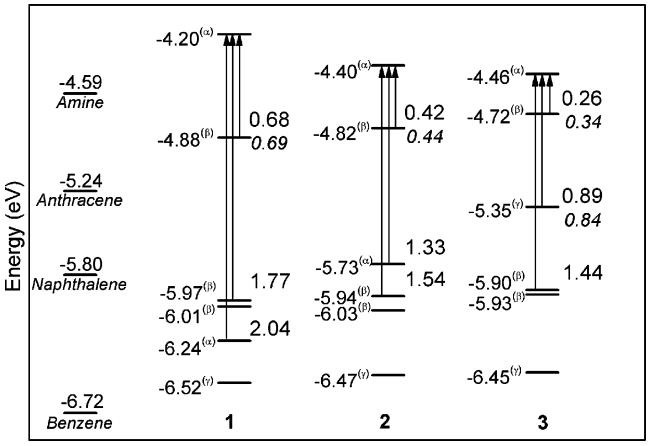

Figure 6. B3LYP/6-31G**-derived HOMO through HOMO-5 molecular orbital energies for compounds **1**, **2**, and **3**, as well as the isolated *N*,*N*-di-(4-methoxyphenyl)amine and bridge components. The molecular orbital energies are labeled with superscripts according to the predominant makeup of the orbital structure (see Figure 7): (α) amine with strong bridge component; (β) mostly amine; and (γ) mostly bridge. The values given in italics represent the energy separation as determined by UPS.

For the AM1/CI method, a number of configuration-interaction spaces were explored. These spaces were first limited to the HOMO, SOMO, and LUMO molecular orbitals of the radical cation; larger configuration-interaction spaces that also included molecular orbitals primarily located on the bridges were then considered. However, no significant differences in the optimized radical-cation structures were found as a function of the size of the configuration-interaction space chosen for the analysis. In all cases, symmetric, charge-delocalized structures consistent with the UB3LYP/6-31G** results were obtained. These results along with the weak solvent dependence of the IV-CT bands strongly point toward the assignment of $\mathbf{1}^+$−$\mathbf{3}^+$ to Robin and Day's Class III or at least to Class III−Class II borderline.

Electronic Structure and Optical Properties. On the basis of the DFT-computed neutral geometries, the Kohn−Sham energies for the upper occupied molecular orbitals (HOMO to HOMO-5) of **1**−**3** are given in Figure 6, together with the energies of the isolated bridge units and the *N*,*N*-di(4-methoxyphenyl)amine group; Figure 7 provides a pictorial representation of the molecular orbitals. While a comparison of the Kohn−Sham orbital energies with those of the UPS measurements indicates that the application of Koopmans' Theorem (KT)[36] leads to absolute IP values that are about 2 eV too low, it is important to note that the energetic splittings between the HOMO and HOMO-1 are in very good agreement with the experimental ΔIP values (see Figure 6).

The molecular orbitals within the HOMO−HOMO-5 range can be classified into three categories according to their relative localizations on the molecular structure:

(i) those lying on both the amine and bridge components,

(ii) those lying predominantly on the amine segments, and

(iii) those lying predominantly on the bridge.

Consistently across the series, the HOMO (see Figure 7) has significant density on both the amine and bridge components while the HOMO-1 lies solely on the amines. In addition, a

(34) Szeghalmi, A. V. et al. *J. Am. Chem. Soc.* **2004**, *126*, 7834−7845.
(35) Bally, T.; Borden, W. T. *Rev. Comput. Chem.* **1999**, *13*, 1−99.
(36) Koopmans, T. *Physica* **1933**, *1*, 104−113.

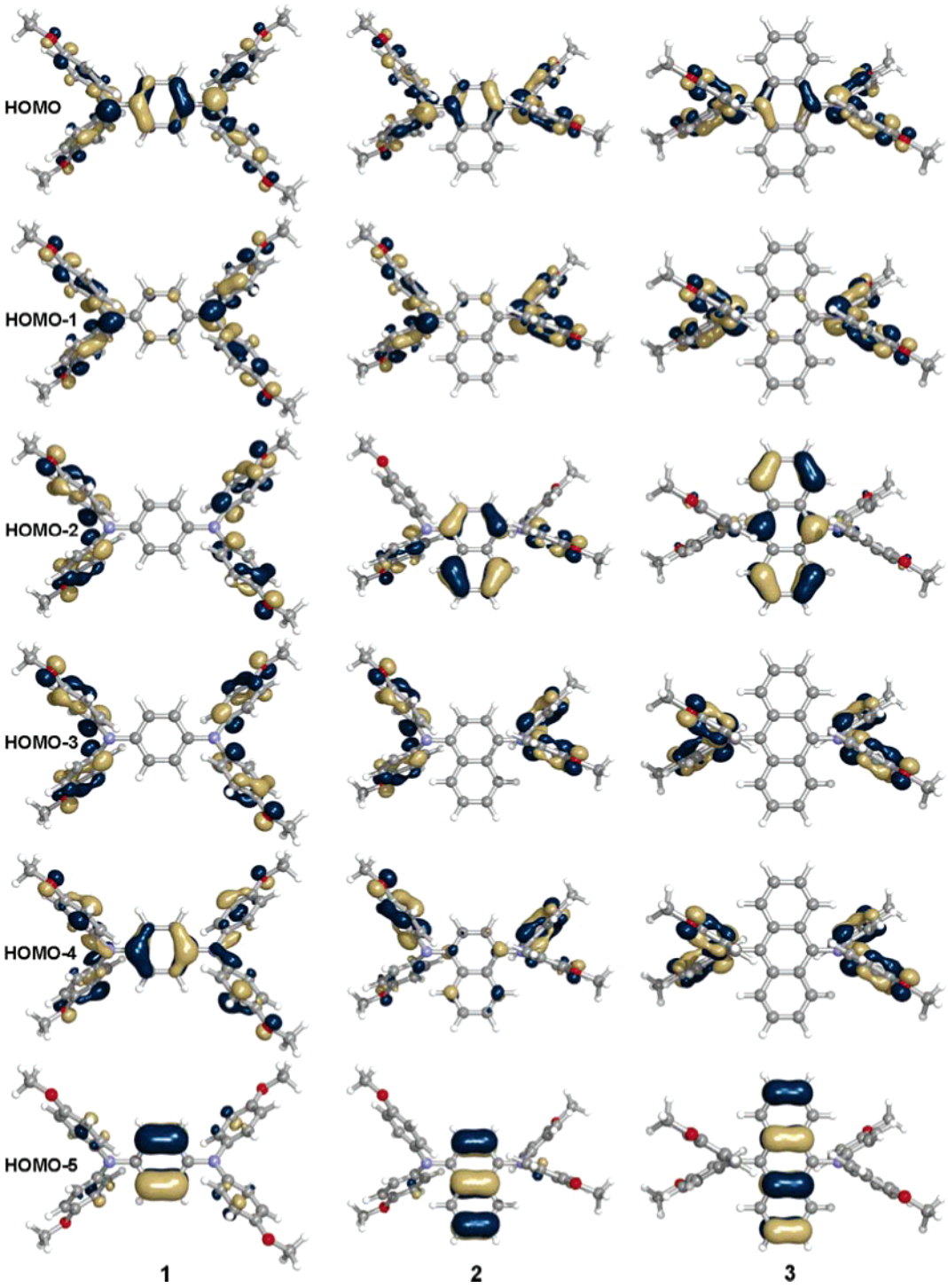

Figure 7. Pictorial representation of the B3LYP/6-31G**-derived HOMO through HOMO-5 molecular orbitals in **1**, **2**, and **3**.

distinction can be made in the energetic ordering of the next set of amine-based and bridge-character orbitals corresponding to HOMO-2 through HOMO-4. For **1**−**3**, there exists a pair of nearly degenerate amine-based molecular orbitals that maintain similar energies (between −6.03 and −5.90 eV) across the series. In **1**, the next bridge-character orbital lies 0.23 eV below this degenerate pair, while in **2** and **3** the bridge-character molecular orbitals are destabilized versus the degenerate amine orbitals (by 0.21 and 0.55 eV, respectively). This picture is in accordance with the UPS data (see Figure 1) that indicate a peak at ca. 8.3 eV for **1**−**3**, which we assign to the amine-based levels, while **2** and **3** have a peak at ca. 7.9 and 7.28 eV, respectively, that we assign to the bridge-character level. In addition to the concurrence in the energetic splitting of the first two ionization potentials determined via simple KT analysis of the molecular orbital eigenvalues and the UPS spectra, there is also excellent agreement found through direct B3LYP/6-31G** calculations of the vertical ionization energies at the ΔSCF level. Though there is an approximate 1 eV discrepancy in the absolute values of the ionization potentials, the energy splittings of 0.65, 0.41, and 0.27 eV obtained for **1**, **2**, and **3**, respectively, are nearly identical to those derived from the UPS spectra and demonstrate the reliability of the simple molecular orbital analysis.

Table 4. TD-DFT Vertical Excitation Energies and Oscillator Strengths [μ] of Systems $\mathbf{1}^+-\mathbf{3}^+$ Obtained at the UB3LYP/6-31G** Radical-Cation Geometry[a]

	$\tilde{\nu}_{abs}$/cm^{-1}	μ/D	configuration
$\mathbf{1}^+$	9290	10.32	HOMO-1 → HOMO (0.87); HOMO → LUMO+1 (0.17)
	15630	2.14	HOMO-2 → HOMO (0.97)
	15900	4.61	HOMO-3 → HOMO (0.97)
	16990	0.00	HOMO-4 → HOMO (0.97)
$\mathbf{2}^+$	7710	9.90	HOMO-1 → HOMO (0.85); HOMO → LUMO (0.19)
	13300	0.72	HOMO-2 → HOMO (0.94); HOMO-4 → HOMO (0.24)
	14820	3.60	HOMO-3 → HOMO (0.96)
	15340	4.01	HOMO-4 → HOMO (0.94); HOMO-2 → HOMO (0.24)
$\mathbf{3}^+$	5730	9.31	HOMO-1 → HOMO (0.80); HOMO → LUMO (0.20)
	9390	0.00	HOMO-2 → HOMO (0.96); HOMO-1 → LUMO (0.10)
	13400	2.49	HOMO-3 → HOMO (0.96)
	13780	4.88	HOMO-4 → HOMO (0.96)

[a] Molecular orbital configurations are labeled in reference to the neutral states.

The relative orderings of these lower molecular orbitals play a significant role in the electronic transitions that are allowed for $\mathbf{1}^+-\mathbf{3}^+$, as confirmed by TD-DFT calculations for the radical cations (see Table 4). For $\mathbf{1}^+-\mathbf{3}^+$, the first excitation corresponds to the CR transition and primarily involves the HOMO-1 → HOMO excitation (the notation for the MOs refers to the neutral ground state). The calculated transition energies agree well with the energies of the experimental optical CR bands (given in Table 3). The next allowed transition in all three systems is predicted to originate from the quasi-degenerate amine-based molecular orbitals (HOMO-2 and HOMO-3 in $\mathbf{1}^+$, HOMO-3 and HOMO-4 in $\mathbf{2}^+$ and $\mathbf{3}^+$). The calculated energies are again in good agreement with experimental data. However, the TD-DFT calculations, in contrast to experiment, predict nearly the same intensity across the series. It is important to mention that, in $\mathbf{1}^+$, the third excited state, which arises from the excitation of the bridge-localized HOMO-4, lies very close to the second (quasi-degenerate) excited state. For $\mathbf{2}^+$ and $\mathbf{3}^+$, where the bridge-based molecular orbital is energetically destabilized versus the degenerate amine-based orbitals, the ordering of the respective excited states is inverted. Thus, in $\mathbf{3}^+$, the bridge-localized excited state is located halfway between the CR and amine-based states. While optical transition to the bridge-localized state is forbidden in the dipole approximation, this state might be responsible for the appearance of different scenarios of vibronic interactions in $\mathbf{1}^+-\mathbf{3}^+$. Therefore, the assignment of the higher-energy bands in these systems and the understanding of the origin of their fine structure require further investigations.

Electronic Coupling. We have employed different methods to evaluate the electronic coupling between the diabatic states in the $\mathbf{1}^+-\mathbf{3}^+$ radical-cation series. The first is based on the fitting of the absorption spectra to a two-level/two-mode model in which the contribution from a symmetric mode is added to the conventional Marcus−Hush asymmetric coordinate (see Figures 1 and 2).[21−23] This approach, which we recently described in detail,[34] is based on a semiclassical treatment of this vibronic model. The results of the fit (reorganization energy parameters λ and L and electronic coupling V) are given in Table 5. While this procedure yields for all three ($\mathbf{1}^+-\mathbf{3}^+$) systems (in CH_2Cl_2) a double-minimum adiabatic potential surface, the associated ET barrier ΔG^* is extremely small, on the order of 40−60 cm^{-1} (which is just a fraction of the thermal energy at room temperature). The electronic coupling V as derived from the vibronic model is somewhat smaller than $\tilde{\nu}_{abs}/2$, the value expected for V in delocalized Class III systems. For the sake of comparison, the estimates of electronic couplings obtained by different methods are collected in Table 6. Overall, the optical data suggest a decrease in electronic coupling by nearly a factor of 2 when the phenylene bridge is replaced by an anthrylene bridge.

Table 5. Reorganization Parameters from an Analysis of the Optical Band Shapes (Measured in CH_2Cl_2) within the Two-Mode Model

/cm^{-1}	$\mathbf{1}^+$	$\mathbf{2}^+$	$\mathbf{3}^+$
l	10000	8200	5200
L	2030	2050	1850
V	4300	3600	2200
ΔG^*	60	40	50

Table 6. Electronic Coupling Parameters (cm^{-1}) as Determined from Koopmans' Theorem Analysis and Experimental UPS and Optical Data

	$\mathbf{1}^+$	$\mathbf{2}^+$	$\mathbf{3}^+$
KT-AM1[a]	2380	1420	950
KT-DFT[a]	2740	1670	1080
UPS (ΔIP/2)	2780	1770	1370
ΔIP/2 + L^*	3800	2960	2160
V[b]	4300	3600	2200
exp. $\tilde{\nu}_{abs}/2$	4740	4000	2570

[a] Evaluations were made with respect to the DFT-optimized neutral geometry. [b] From band fitting, see Table 5.

Another important result obtained from the absorption data is related to the reorganization energy λ. As seen from Table 5, λ also decreases by a factor of 2 when going from $\mathbf{1}^+$ to $\mathbf{3}^+$. Thus, the $2V/\lambda$ ratio retains a value close to 1 along the series. This result is in agreement with our earlier assignment for $\mathbf{1}^+-\mathbf{3}^+$ as being borderline Class III/Class II systems. However, in itself, the significant decrease in λ is unexpected. Indeed, the physical origin of λ is found in the pseudo Jahn−Teller interaction between the diabatic delocalized electronic states: $\Psi_+ = (1/\sqrt{2})(\Psi_a + \Psi_b)$ and $\Psi_- = (1/\sqrt{2})(\Psi_a - \Psi_b)$. Since the energy difference between these states decreases as we go from phenylene to anthrylene bridges, an opposite trend would be expected for the pseudo Jahn−Teller vibronic interactions and, consequently, for the evolution of λ. Therefore, further investigations of the vibronic interactions are required to shed more light on this issue.

The second experimental estimate of electronic coupling has been obtained from the UPS measurements. We have shown recently[31] that the first and second IPs correspond to the formation of the *delocalized* electronic states of the radical cation Ψ_+ and Ψ_-; thus, ΔIP gives a direct estimate of the electronic

Table 7. Intramolecular Reorganization Energies and Correction (L^*) Obtained at the UB3LYP/6-31G** Level

/cm^{-1}	λ_1	λ_2	L	L^*
1	1090	1200	2160	1020
2	1340	1190	2240	1190
3	940	780	1430	790

coupling 2V. As seen from Tables 1 and 6, the UPS estimates, as well as those derived from the optical bands, point to a large decrease in V when going from $\mathbf{1}^+$ to $\mathbf{3}^+$. The UPS values of ΔIP are smaller than the 2V values derived from the optical spectra. The discrepancy between the two sets of data is related to the fact that ΔIP is determined at the geometry (see Figure 2) of the neutral molecule. Thus, the UPS measurements provide a lower bound of the electronic coupling. To obtain more accurate estimates of V, the ΔIP/2 values should be corrected to account for the relaxation effects that take place on going from neutral to radical-cation states. The most accurate way to accomplish that correction would be to fit the shape of the ionization spectrum to a vibronic coupling model. However, a simple correction can be obtained in the framework of an adiabatic approximation. According to Figure 2, we can write:

$$V = (\Delta\mathrm{IP}/2) + L^*$$

$$L^* = {}^1/_2(L + \lambda_1 - \lambda_2)$$

Here, λ_1 and λ_2 are the relaxation energies of the ground state and first excited state of the radical cation with respect to the geometry of the neutral ground state. The estimated relaxation energies are given in Table 7. As seen from Table 7, the values of L for $\mathbf{1}^+$ and $\mathbf{2}^+$ are similar and significantly larger than those for $\mathbf{3}^+$. These differences arise from the extent of geometry modifications observed upon excitation of the radical-cation species: changes in both the carbon−nitrogen bonds and torsional orientations of the 4-methoxyphenyl groups are dramatically larger for $\mathbf{1}^+$ and $\mathbf{2}^+$ than those observed in $\mathbf{3}^+$ (see Table S4 in the Supporting Information).

Previously,[31] we approximated L^* with L, assuming that the geometry in the cation excited state is similar to that in the neutral ground state. The calculations of the relaxation energies show, however, that L^* is more likely to be equal to about half of L for these systems. The UPS values of V corrected by L^*, while still on the small side, are now in good agreement with those derived from the analysis of the CR bands.

Thus, as seen from Table 6, both experimental measurements and electronic-structure calculations concur to demonstrate that the anthracene bridge provides for a significantly smaller electronic coupling than the benzene bridge. We interpret this finding as a result of the influence of steric interactions on the super-exchange mechanism. We believe that these interactions control the electronic communication between the redox centers in $\mathbf{1}^+$−$\mathbf{3}^+$. For a complete description of the super-exchange interaction, we would need to take the bridge levels explicitly into consideration, preferably by using many-state models. Here, for the purpose of providing a simple, qualitative explanation, we discuss the results obtained in the framework of perturbation theory. If we assume, for the sake of simplicity, that a single pathway contributes to the super-exchange interaction (that likely operates via occupied bridge levels, as they are energetically (see Figure 6) the most favorable), the electronic coupling V can be approximated in the tight-binding approximation as:[37]

$$V = \frac{V_B^2}{\Delta E}$$

Here, V_B is the electronic coupling between the redox site and the bridge, and ΔE is the energy gap between the relevant states. Since V_B strongly depends on the mutual orientations of the bridge and redox unit, an unfavorable orientation between these two units will diminish the gain in electronic coupling obtained from the decrease in ΔE. For $\mathbf{1}^+$, the twist angle with respect to the bridge is 27°, while for $\mathbf{3}^+$, the twist angle is 62°. Thus, the smaller twist angles in $\mathbf{1}^+$ allow for a stronger interaction and larger V. The large twist angle in $\mathbf{3}^+$ significantly reduces the electronic coupling despite a large reduction in ΔE in $\mathbf{3}^+$ with respect to $\mathbf{1}^+$ (see Figure 6). If the orientations of the p-methoxyphenyl groups in $\mathbf{3}^+$ are forced to be the same as those in $\mathbf{1}^+$, the KT estimate of the electronic coupling in $\mathbf{3}^+$ (0.42 eV) is similar to that determined for $\mathbf{1}^+$ (0.48 eV), revealing a significant increase with respect to the value of 0.23 eV found for the optimized geometry of $\mathbf{3}^+$. This illustrates that the electronic coupling in $\mathbf{1}^+$−$\mathbf{3}^+$ is largely dominated by steric interactions between the p-methoxyphenyl groups and the bridge. In addition, we suggest that a second effect that limits the strength of the electronic coupling in $\mathbf{2}^+$ and $\mathbf{3}^+$ is related to the nonplanarity of the naphthylene and anthrylene bridges in these systems.

The situation is strikingly different in the case of systems with 1,4-diethynylbenzene and 9,10-diethynylanthracene spacers similar to the **L1** and **L2** molecules sketched below. As described previously,[6,7,14,15] the presence of ethynylene units removes the steric interactions between the amino and arylene units and preserves the planarity of the central unit. As expected, the decrease in energy gap ΔE in **L2** with respect to **L1** now results in an enhancement of the electronic communication.[6−8,14,15]

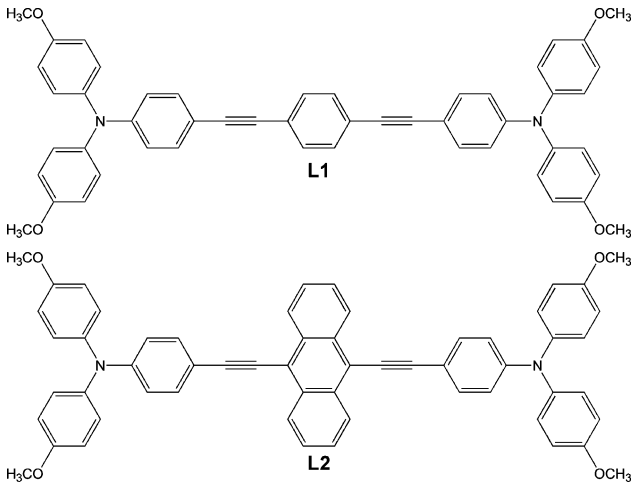

IV. Synopsis

In this work, we have investigated the electronic interactions in three organic mixed-valence systems $\mathbf{1}^+$−$\mathbf{3}^+$ that present similar bridge lengths. The electronic coupling has been estimated by means of gas-phase ultraviolet photoelectron spectroscopy, vis/NIR spectroscopy, and electronic-structure

(37) Creutz, C.; Newton, M. D.; Sutin, N. *J. Photochem. Photobiol., A* **1994**, *82*, 47−59.

calculations. The optical data point toward the assignment of $\mathbf{1}^{+}-\mathbf{3}^{+}$ as Class III or borderline Class III/Class II MV systems. Our work provides a first example where an anthracene bridge is found to be less effective than a benzene bridge in mediating the electronic communication between redox centers. Our results suggest that the electronic coupling is controlled by a subtle balance between the effects related to the energetics of the bridge and the redox units and to the topology of the bridge-redox center segment.

Acknowledgment. The work at the Georgia Institute of Technology was supported by the National Science Foundation through the STC Program under Award Number DMR-0120967 and Grant CHE-0342321, and by the IBM Shared University Research Program. The work in Würzburg was supported by the Deutsche Forschungsgemeinschaft and Degussa AG.

Supporting Information Available: Details of the synthesis, the procedure for the acquisition of the experimental data, the description of the X-ray structure determination of **3**, results of the electronic-structure calculations at the DFT and AM1 levels, and full citation for References 30 and 34 (PDF, CIF). This material is available free of charge via the Internet at http://pubs.acs.org.

JA0512172